Available online at www.sciencedirect.com

ScienceDirect

Geochimica et Cosmochimica Acta 308 (2021) 173–187

Geochimica et Cosmochimica Acta

www.elsevier.com/locate/gca

Variable refractory lithophile element compositions of planetary building blocks: Insights from components of enstatite chondrites

Takashi Yoshizaki [a,*], Richard D. Ash [b], Marc D. Lipella [b,1], Tetsuya Yokoyama [c], William F. McDonough [a,b,d]

[a] *Department of Earth Science, Graduate School of Science, Tohoku University, Sendai, Miyagi 980-8578, Japan*
[b] *Department of Geology, University of Maryland, College Park, MD 20742, USA*
[c] *Department of Earth and Planetary Sciences, Tokyo Institute of Technology, Ookayama, Tokyo 152-8851, Japan*
[d] *Research Center of Neutrino Sciences, Tohoku University, Sendai, Miyagi 980-8578, Japan*

Received 17 November 2020; accepted in revised form 31 May 2021; available online 8 June 2021

Abstract

Chondrites are sediments of materials left over from the earliest stage of the solar system history. Based on their undifferentiated nature and less fractionated chemical compositions, chondrites are widely considered to represent the unprocessed building blocks of the terrestrial planets and their embryos. Models of chemical composition of the terrestrial planets generally find chondritic relative abundances of refractory lithophile elements (RLE) in the bulk bodies ("constant RLE ratio rule"), based on limited variations of RLE ratios among chondritic meteorites and the solar photosphere. Here, we show that ratios of RLE, such as Nb/Ta, Zr/Hf, Sm/Nd and Al/Ti, are fractionated from the solar value in chondrules from enstatite chondrites (EC). The fractionated RLE ratios of individual EC chondrules document different chalcophile affinities of RLE under highly reducing environments and a separation of RLE-bearing sulfides from silicates before and/or during chondrule formation. In contrast, the bulk EC have solar-like RLE ratios, indicating that a physical sorting of silicates and sulfides was negligible before and during the accretion of EC parent bodies. Likewise, if the Earth's accretion was dominated by EC-like materials, as supported by multiple isotope systematics, physical sorting of silicates and sulfides in the accretionary disk did not occur. Alternatively, the Earth's precursors were high-temperature nebular condensates that formed prior to the precipitation of RLE-bearing sulfides. A lack of Ti depletion in the bulk silicate Earth, combined with similar silicate-sulfide and rutile-melt partitioning behaviors of Nb and Ti, prefers a moderately siderophile behavior of Nb as the origin of the accessible Earth's Nb depletion. Highly reduced planets that have experienced selective removal or accretion of silicates or metal/sulfide phases, such as Mercury, possibly yield fractionated, non-solar bulk RLE ratios.

Keywords: Planets; Chondrites; Earth; Refractory lithophile elements; Chemical fractionation

1. INTRODUCTION

The geochemical classification of elements is based on their partitioning behaviors during condensation into a silicate (lithophile), metal (siderophile) or sulfide (chalcophile) phases (e.g., Lodders, 2003). Elements are also classified

* Corresponding author.
E-mail address: tky@dc.tohoku.ac.jp (T. Yoshizaki).
[1] Deceased.

https://doi.org/10.1016/j.gca.2021.05.057
0016-7037/

cosmochemically based on their volatilities under assumed redox conditions. There are 36 refractory elements, most are lithophile (e.g., Be, Al, Ca, Ti, Sc, Sr, Y, Zr, Nb, Ba, rare earth elements (REE), Hf, Ta, Th and U), while V, Mo, and W are moderately siderophile/chalcophile, and Ru, Rh, Re, Os, Ir, and Pt are highly siderophile. Chondritic meteorites (chondrites) are undifferentiated solar system materials that are widely considered as planetary building blocks. The relative abundances of the most refractory lithophile elements (RLE) are nearly constant ($\lesssim$ 10%) for the solar photosphere and among chondritic meteorites (Larimer and Wasson, 1988; Wasson and Kallemeyn, 1988; Bouvier et al., 2008). Importantly, compositional models of Earth (Allègre et al., 1995; McDonough and Sun, 1995; Palme and O'Neill, 2014) and Mars (Wänke and Dreibus, 1994; Yoshizaki and McDonough, 2020) commonly find or assume chondritic RLE ratios (e.g., Ca/Al, Sm/Nd, Lu/Hf, Th/U) for these planets ("constant RLE ratio rule").

However, recent high-precision measurements of chondritic and terrestrial samples revealed detectable variations of not only REE ratios (Dauphas and Pourmand, 2015; Barrat et al., 2016), but also geochemical twins' ratios such as Y/Ho (Pack et al., 2007), Zr/Hf (Patzer et al., 2010), and Nb/Ta (Münker et al., 2003) among solar system materials. For example, the a low Nb/Ta value for the accessible Earth, as compared to CI chondrites, which show the closest match to the solar photosphere composition (e.g., Lodders, 2020), raised discussion on their relative non-lithophile behaviors. Some authors proposed that Nb and Ta are exclusively lithophile and hosted in an eclogitic reservoir hidden in the mantle (Sun and McDonough, 1989; McDonough, 1991; Kamber and Collerson, 2000; Rudnick et al., 2000; Nebel et al., 2010), whereas others have suggested that Nb and less so Ta behaved as moderately siderophile (Wade and Wood, 2001; Münker et al., 2003; Corgne et al., 2008; Mann et al., 2009; Cartier et al., 2014) or chalcophile (Münker et al., 2017) elements and may have been partially sequestered into the Earth's core.

The Earth's specific building blocks remain unknown. Among chondritic meteorites, enstatite chondrites (EC) show the closest isotopic match to the Earth's mantle (Javoy et al., 2010; Warren, 2011; Dauphas, 2017; Boyet et al., 2018). On the other hand, EC have lower Mg/Si and RLE/Mg ratios and higher volatile abundances as compared to Earth (Palme et al., 1988; McDonough and Sun, 1995). EC are an uncommon type of chondrite in our meteorite collection that record the most reducing conditions among chondritic meteorites (Fig. 1; Keil, 1968; Larimer, 1968). The chemical and isotopic composition of meteorites and Earth, combined with partitioning behaviors of elements, indicate that an early stage of the Earth's formation was dominated by an accretion of EC-like, highly reduced materials, followed by an accretion of less reduced ones (e.g., Corgne et al., 2008; Mann et al., 2009; Schönbächler et al., 2010; Rubie et al., 2011; Rubie et al., 2015). Multiple RLE show non-lithophile behavior under highly reduced conditions, as recorded in EC (e.g., Barrat et al., 2014; Münker et al., 2017), but these attributes of RLE have not been linked to the Earth's composition.

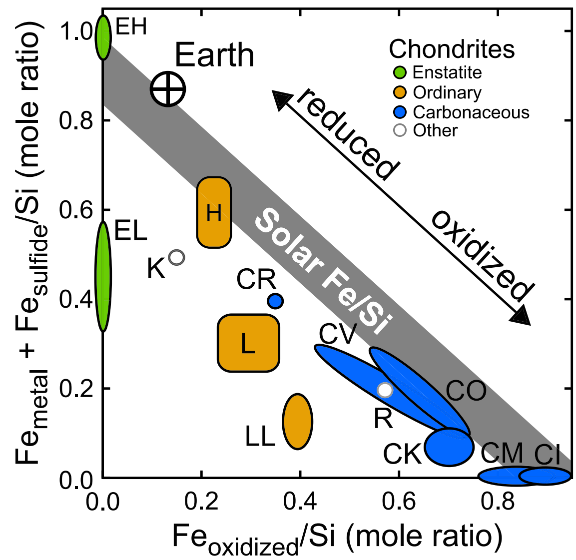

Fig. 1. The Urey-Craig diagram showing variation in oxidation state of iron relative to silicon among chondrite groups (after Urey and Craig, 1953). The plot of Earth is based on McDonough (2014). Metal-rich CB and CH chondrites are not included in the plot because their origin (condensation from a gas-melt plume formed by a planetary-scale collision; e.g., Krot et al., 2012) is distinct from that of major chondrite groups.

Here, we report RLE composition of chondrules, a major RLE carrier in chondritic meteorites (e.g., Alexander, 2005; Alexander, 2019a; Alexander, 2019b) and potentially the dominant source material for the terrestrial mantle (e.g., Hewins and Herzberg, 1996; Johansen et al., 2015; Levison et al., 2015; Amsellem et al., 2017; Yoshizaki and McDonough, in press). We also report RLE compositions of sulfides from primitive EC samples and reveal the non-lithophile behavior of some RLE in highly reducing environments. Using these and published data, combined with some new RLE data for refractory inclusions from carbonaceous chondrites (CC), we examine the compositional variability in RLE ratios within the accretionary disk, the behavior of elements under variable redox conditions, and the chondritic reference frame for bulk planetary compositions.

2. SAMPLES AND METHODS

2.1. Samples

In order to reduce potential modifications of elemental abundances by parent body metamorphism and terrestrial weathering, we chose unequilibrated (type 3) EH, EL and CV chondrites with limited terrestrial weathering as samples for this study (Table 1). Analyses were conducted on 92 chondrules, 40 troilites (FeS), 9 oldhamites (CaS) and 5 niningerites (MgS) from Alan Hills (ALH) A77295 (EH3), ALH 84170 (EH3), ALH 84206 (EH3), ALH 85119 (EL3) and MacAlpine Hills (MAC) 88136 (EL3). We also studied two Ca, Al-rich inclusions (CAI) from Allende (CV3), and one CAI and six amoeboid olivine aggregates (AOA) from

Table 1
List of meteorite samples used in this study. Meteorite types and weathering grades are based on the online Meteoritical Bulletin Database (www.lpi.usra.edu/meteor/) and Satterwhite and Righter (2007). Abbreviations: NIPR–National Institute of Polar Research; SI–Smithsonian Institution.

Name	Type	Weathering grade	Sample source
ALHA77295	EH3	B	NIPR
ALH 84206	EH3	A/B	NASA/JSC
ALH 84170	EH3	B	NASA/JSC
MAC 88136	EL3	A	NASA/JSC
ALH 85119	EL3	Be	NASA/JSC
RBT 04143	CV3	B	NASA/JSC
Allende	CV3	Fall	SI

Roberts Massif (RBT) 04143 (CV3). The petrology and mineralogy of these meteorites have been well characterized in previous studies (e.g., Johnson and Lofgren, 1995; Rubin et al., 1997; Benoit et al., 2002; Lin and El Goresy, 2002; Grossman and Brearley, 2005; Gannoun et al., 2011; Quirico et al., 2011; Ishida et al., 2012; Yoshizaki et al., 2019; Bonal et al., 2020).

2.2. Analytical methods

Mineralogy, petrology and major element compositions of polished sections of the samples were analyzed using scanning electron microscopes (SEM) and electron probe microanalyzers (EPMA) at Tohoku University and University of Maryland, using procedures after Yoshizaki et al. (2019, Section B.1). Trace element compositions of chondritic components were determined using a New Wave frequency-quintupled Nd:YAG laser system coupled to a Thermo Finnigan Element2 single-collector ICP-MS at University of Maryland, following procedures of Lehner et al. (2014). Operating conditions are summarized in Table 2. Measurements were carried out in low-mass resolution mode ($M/\Delta M = 300$), with 15–200 μm laser spot size and a fluence of ~2–3 J/cm^2. In all circumstances, the spot size was set to be smaller than the chondrule so that the laser sampled only the polymineralic interiors of chondrules. Time-resolved spectra were also used to confirm that the analyses were restricted to the chondrule. The beam was focused onto a sample placed in a 3 cm^3ablation cell, which was continuously flushed to the plasma source of the mass spectrometer with a He gas flow of ~1 L/min. The mass spectrometer was tuned to maximize signal (based on ^{43}Ca and ^{232}Th spectra) and minimize oxide production ($UO/U < 1.2\%$) to maximize sensitivity and reduce polyatomic interference. A dwell time of 5–15 ms was used depending on element concentrations. After the LA-ICP-MS measurements, the sampled areas were investigated using SEM, to make sure that there was no contamination due to beam overlapping onto neighboring phases (e.g., matrix).

In LA-ICP-MS measurement of chondrules and refractory inclusions, National Institute of Standards and Technology (NIST) 610 glass (Jochum et al., 2011) was used as an external standard material. Internal standards were ^{29}Si for chondrules, and ^{29}Si, ^{43}Ca or ^{47}Ti for refractory inclusions, which were determined as a polymineralic bulk composition using EPMA. For sulfides, the group IIA iron meteorite Filomena (for siderophile elements) and the

Table 2
Conditions of the LA-ICP-MS measurement.

Thermo Finnigan Element2 single-collector, sector field ICP-MS	
Forward power	1265 W
HV	8 kV
Number of pre-scans	1
Active dead time	18 ns
Cool gas flow	16 L/min Ar
Auxiliary gas flow	1.05 L/min Ar
Sample gas flow	1.040 L/min Ar
Autosampler	ASX-100 (CETAC Technologies)
Torch	Quartz
Injector	Quartz
Skimmer cone	Al-alloy
Sampling cone	Al-alloy
Detection mode	Analogue or both
Dwell time	20 s background acquisition, 40 s data acquisition
Samples/peak	1
Runs*passes	100*1
Search window	150%
Integration window	80%
Integration type	Intensities
Scan type	EScan
Oxide forming rate	$^{238}U^{16}O/^{238}U$ <2.0%
Electro Scientific New Wave frequency-quintupled Nd:YAG laser (213 nm) system	
Ablation pattern	Spot
Spot diameter	15–200 μm
Repetition rate	7 Hz
Energy density	2–3 J/cm^2

NIST 610 glass (for lithophile elements) were used as reference materials, using data from Walker et al. (2008) and the GeoReM database (Jochum et al., 2011) as working values, respectively. Count rates were normalized using ^{57}Fe (for Filomena) and ^{63}Cu (for NIST 610) as internal standards, which were determined using EPMA or SEM/EDS. The standard materials were measured at least twice at the start and end of individual analytical run composed of 16 analyses of unknown samples. All obtained data were processed using the LAMTRACE software (van Achterbergh et al., 2001). Spectral data with a potential beam overlapping onto neighboring phases were rejected in this procedure. The long-term reproducibilities of isotope ratios for the external standards were better than 5% for nearly all of the measured elements, except for Ni and Cu in Filomena (Table B.1). We also routinely measured the BHVO-2G glass as a secondary standard material to monitor accuracy of the analysis, which reproduced the preferred values (Jochum and Nohl, 2008) within <5%. We report mean ±2 standard errors of the mean ($2\sigma_m$) of RLE ratios of EC chondrules, EC sulfides, and CC refractory inclusions, as a measure of their average RLE ratios.

3. RESULTS

3.1. Chondrules from unequilibrated enstatite chondrites

Various types of chondrules are identified and measured in this study. More than 70% of them are porphyritic pyroxene (PP) chondrules, with less abundant (∼15%) radial pyroxene (RP), olivine-bearing (porphyritic olivine pyroxene (POP) or porphyritic olivine (PO) type; ∼10%), and other rare types (Fig. 2 and 3). These chondrules are mostly 200–600 µm in diameter, with some reaching up to 1 mm. The observed abundance of chondrule types and their size distributions are consistent with previous reports (e.g., Jones, 2012; Weisberg and Kimura, 2012; Jacquet et al., 2018).

PP chondrules are mainly composed of Fe-poor (<2 wt %) enstatite and mesostasis, with minor silicates such as olivine and silica, as reported previously (e.g., Weisberg and Kimura, 2012; Jacquet et al., 2018). These chondrules sometimes contain small amounts of opaque phases, such as Si-bearing Fe-Ni metal, troilite, oldhamite, niningerite (only in EH3) and alabandite (MnS; only in EL3). Although each PP chondrule shows variable lithophile element abundances, with absolute RLE enrichment factors of 0.5–2 ×CI (Fig. 2A–E), their average compositions are similar in each sample (Fig. 2F). On average, PP chondrules are characterized by depletions of REE, Y, high-field strength elements (HFSE: Ti, Zr, Hf, Nb, Ta), Cr, Mn and K compared to Al, Mg and Si. REE and HFSE are also fractionated within these groups; Eu and Yb are depleted compared to other REE, and Zr and Nb show stronger depletions than their geochemical twins, Hf and Ta, respectively. One PP chondrule from MAC 88136 (C14) has numerous tiny grains of oldhamite in its glassy area, which might have contributed to its elevated bulk REE and Y abundances.

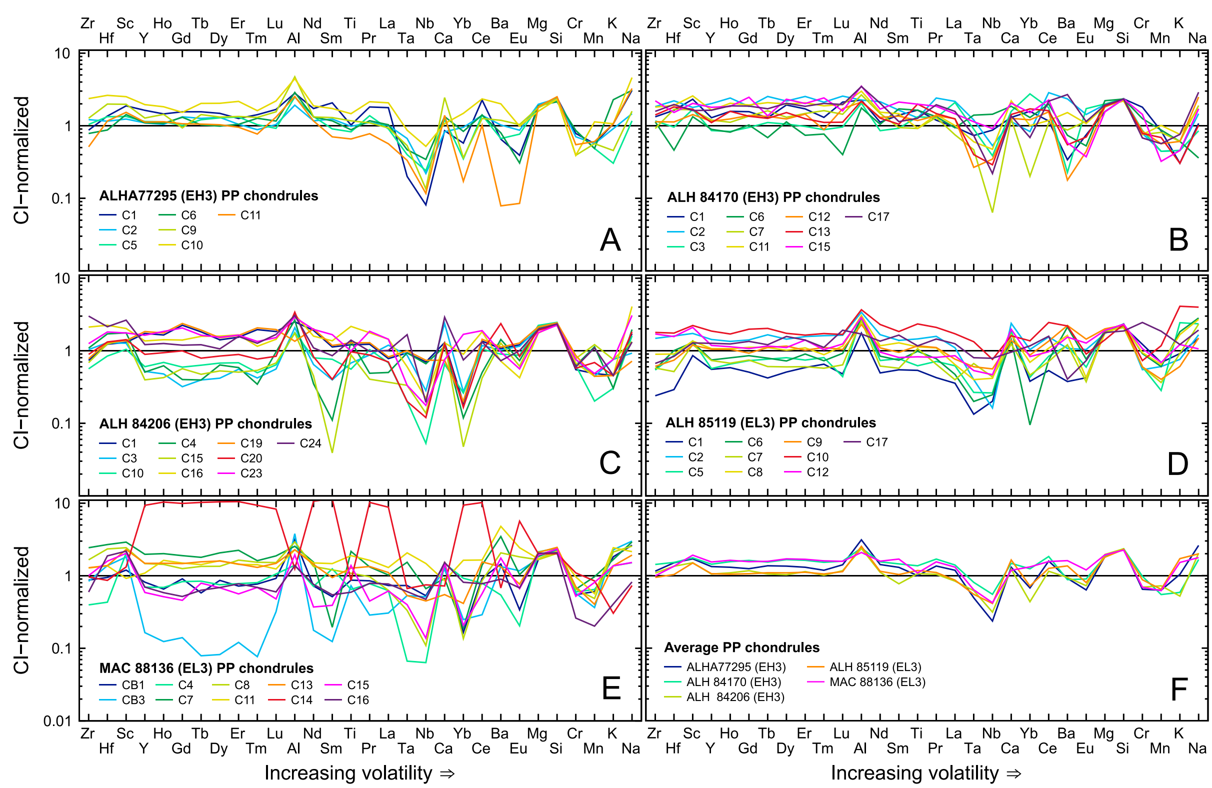

Fig. 2. (A–E) CI-normalized (Lodders, 2020) abundances of lithophile elements in selected porphyritic pyroxene (PP) chondrules from unequilibrated enstatite chondrites, and (F) average composition of PP chondrules in each sample.

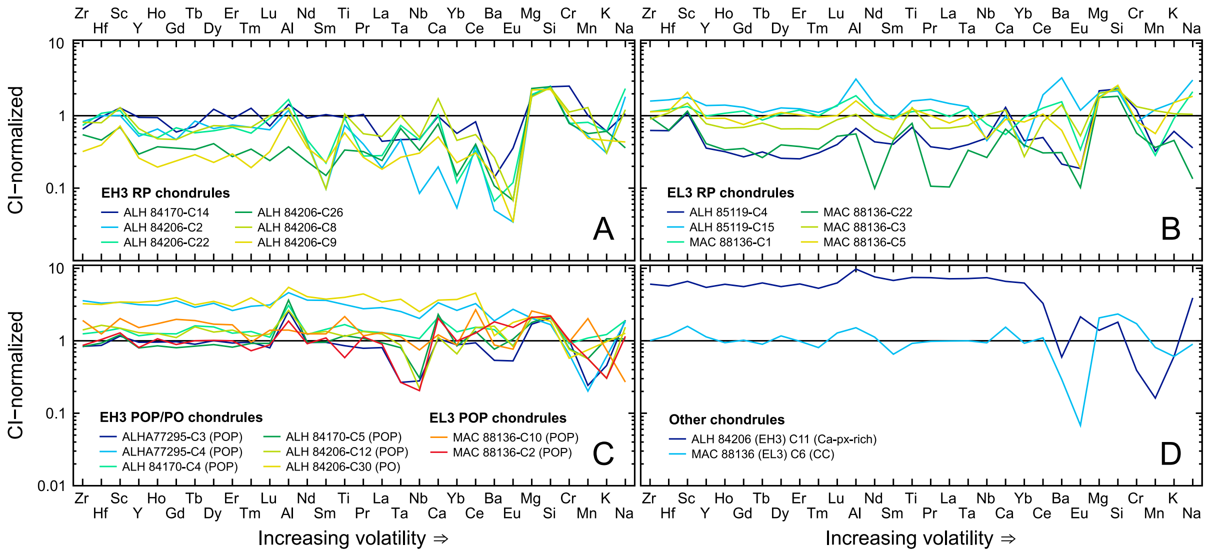

Fig. 3. CI-normalized (Lodders, 2020) abundances of lithophile elements in non-PP chondrules from unequilibrated enstatite chondrites. Abbreviations: CC–cryptocrystalline; PO–porphyritic olivine; POP–porphyritic olivine pyroxene; RP–radial pyroxene.

Compared to PP chondrules, RP chondrules show lower RLE abundance (0.2–1 ×CI; Fig. 3A,B), whereas PO and POP chondrules have higher RLE abundances (0.8–4 ×CI; Fig. 3C). One cryptocrystalline chondrule shows flat RLE pattern with a strong negative Eu anomaly and Al, Mg and Si enrichments (Fig. 3D). In general, RP, olivine-bearing, and cryptocrystalline chondrules are enriched in Al, Mg and Si compared to most RLE, Cr, Mn and K, as observed in PP chondrules. These compositional variations may be affected by sectioning effects (see Section B.2). A Ca-px-rich chondrule in ALH 84206 shows a flat, elevated RLE pattern (~6 ×CI), with depletions of Ce, Ba, Cr, Mn and K (Fig. 3D). In addition, EC chondrules have low Mg/Si (0.84 ± 0.01, $2\sigma_m$), which is as compared to CI (0.89; Lodders, 2020) and the bulk silicate Earth (BSE) (1.1; McDonough and Sun, 1995; Palme and O'Neill, 2014).

EC chondrules show highly variable, fractionated ratios for multiple RLE pairs (Figs. B.3 and 4). Their RLE ratios are not clearly related to their petrological types (e.g., PP, PO, POP). The most significantly fractionated ratios involve Nb relative to other RLE, with average Nb/Ta (13.4 ± 1.6, $2\sigma_m$) and Nb/La (0.691 ± 0.131, $2\sigma_m$) being ~30% and ~40% lower than the CI ratios (~19 and ~1.1; Münker et al., 2003; Barrat et al., 2012; Braukmüller et al., 2018; Lodders, 2020), respectively. EC chondrules, on average, also show lower Zr/Hf (30.0 ± 1.5, $2\sigma_m$), Sm/Nd (0.281 ± 0.021, $2\sigma_m$) and Ca/Al (0.848 ± 0.061, $2\sigma_m$) values, and elevated Al/Ti (33.3 ± 3.1, $2\sigma_m$) as compared to the CI values (i.e., −12%, −15%, −20% and +75% relative to CI, respectively). On the other hand, the average Y/Ho (geochemical twins) in EC chondrules (25.8 ± 0.7, $2\sigma_m$) overlaps the CI composition.

The bulk composition of individual chondrules derived by surface analytical methods (i.e., broadened or scanning beam measurements on thin or thick sections) may be less accurate than that determined by a whole-rock measurement of mechanically separated chondrules (see Section B.2). However, we do not find evidence in our data for such effects. Our data for Nb/La, Zr/Hf, Al/Ti, and Ca/Al in EC chondrules are consistent with EH4 chondrule compositions from Gerber (2012), who measured elemental abundances of solutions of mechanically isolated individual chondrules using ICP-MS and ICP-OES. Slightly elevated Y/Ho and Sm/Nd value for EH4 chondrules reported in Gerber (2012) might reflect distinct behavior of these elements during thermal processing in the EC parent bodies (Barrat et al., 2014). Thus, our surface analyses methods provide bulk EC chondrule compositional data consistent with earlier results that used comparable methods (Grossman et al., 1985; Schneider et al., 2002; Varela et al., 2015). Further discussions on the comparison of data obtained in this and previous studies are provided in Section B.2.

3.2. Sulfides from unequilibrated enstatite chondrites

Both EH3 and EL3 chondrites contain abundant opaque nodules with a range of mineralogies. They are commonly composed of Si-bearing Fe-Ni metal and troilite, with minor occurrence of exotic sulfides including oldhamite, daubréelite ($Fe^{2+}Cr_2^{3+}S_4$), niningerite (in EH3), alabandite (in EL3), K-bearing sulfides, and phosphides. We report only trace element abundances of EC sulfides which occur outside of EC chondrules, whereas those found within chondrules are tiny (mostly <10 μm), making analysis by LA-ICP-MS impractical.

Troilites from primitive EC contain RLE (e.g., Ti (2–7 ×CI), Nb (mostly 0.1–5 ×CI) and Zr (up to 0.2 ×CI)) and nominally chalcophile Cr, Mn and V (Fig. 5; see also Section B.3). In contrast, Ta and Hf, which are geochemical twins of Nb and Zr, respectively, were not detected in the EC troilites. Oldhamites in EC are enriched in multiple RLE, including Zr, Hf, Y, REE, Th and U (Fig. B.4). Most oldhamites show nearly flat REE pattern at 10–100 times higher concentrations than CI, with slightly positive Eu and Yb anomalies in those from EH. They show Zr/Hf (40–600) higher than CI, and variable Sm/Nd (0.34 $\pm$ 0.11, $2\sigma_m$), Y/Ho (31 $\pm$ 7, $2\sigma_m$) and Th/U (4.5 $\pm$ 2.5, $2\sigma_m$) values, which are generally consistent with data reported in Gannoun et al. (2011). Niningerites in EH are enriched in Sc (2–12 ×CI) and Zr (0.2–16 ×CI) (Table E.3). Aluminum was undetectable in nearly all sulfides measured, indicating that it is lithophile under highly reducing conditions.

3.3. Refractory inclusions from unequilibrated carbonaceous chondrites

CAI and AOA from CV chondrites have highly fractionated RLE compositions (Figs. B.5 and B.6; see also Section B.4), reflecting their volatility-driven fractionation during their condensation (e.g., Boynton, 1975). Their RLE compositions are generally consistent with previous studies (e.g., Boynton, 1975; Mason and Martin, 1977; Kornacki and Fegley, 1986; Stracke et al., 2012; Patzer et al., 2018, and references therein). CAI and spinel-rich AOA show low Nb/Ta ratios (3–10), whereas olivine-rich AOA have higher values (18–37). Fractionated Zr/Hf (mostly 33–55), Y/Ho (17–38), and Sm/Nd (0.12–0.54) values are found in CAI and AOA from CV chondrites.

4. DISCUSSION

4.1. RLE fractionation under reduced conditions

Ratios of RLE in individual chondrules from EC, OC, and CC provide insights into the distribution of these elements and chemical fractionation processes occurring in the accretionary disk. Although chondrules show considerable scatter in RLE ratios (Fig. 4), their mean compositions provide a measure of distinction between each chondrite class (EC, OC, and CC), reflecting limited mixing of distinct chondrule reservoirs (e.g., Clayton, 2003; Hezel and Parteli, 2018). Here we propose that RLE fractionation processes recorded in highly reduced EC chondrules are distinct from those in less reduced OC and CC chondrules.

Incomplete high-temperature condensation from the gas of solar composition fractionated RLE, as recorded in CAI and AOA (Fig. B.5; e.g., Boynton, 1975; Kornacki and Fegley, 1986; Ruzicka et al., 2012). The analyzed CAI and Ca, Al-rich AOA have Nb/Ta values ranging from 3 to 10 (Fig. B.6) and are lower than the CI value. In contrast, olivine-rich, less refractory AOA do not show such low Nb/Ta ratios. The low Nb/Ta ratios might reflect Nb-Ta fractionation during formation of high-temperature nebular condensates due to different condensation temperatures of these geochemical twins (1559 K and 1573 K for Nb and Ta, respectively) (Lodders, 2003; Münker et al., 2003). Similarly, higher half-mass condensation temperatures for Zr and Y, as compared to their geochemical twins Hf and Ho, respectively, may produce condensates with non-CI Zr/Hf and Y/Ho ratios (Figs. B.5 and B.6B,E; El Goresy et al., 2002; Pack et al., 2007; Patzer et al., 2010; Patzer et al., 2018; Stracke et al., 2012). The non-CI Nb/Ta, Zr/Hf and Y/Ho values in bulk OC and CC chondrites have been attributed to additions of the refractory materials with fractionated RLE compositions into OC and CC asteroids (Münker et al., 2003; Pack et al., 2007; Patzer et al., 2010; Stracke et al., 2012). Likewise, these additions might also be responsible for chondrules possessing similar fractionated Nb/Ta and Zr/Hf ratios (e.g., Misawa and Nakamura, 1988; Misawa and Nakamura, 1988; Pack et al., 2004; Patzer et al., 2018). In contrast, the CI-like average Y/Ho in OC and CC chondrules indicate a similar behavior of these geochemical twins during formation of these chondrules and their precursors (Pack et al., 2007).

Compared to OC and CC chondrules, EC chondrules show more distinct differences in key RLE ratios (e.g., Nb/Ta, Nb/La, Zr/Hf, Sm/Nd, Al/Ti, Ca/Al; Figs. 4 and B.3). Importantly, most RLE are depleted relative to Al in EC chondrules (e.g., super-CI Al/Ti and sub-CI Ca/Al); this feature is distinct from CI-like RLE/Al values in OC and CC chondrules (Fig. 2–4). These differences indicate that RLE fractionation processes recorded in EC chondrules differ from those of OC and CC chondrules (i.e., volatility-driven fractionation; Misawa and Nakamura, 1988; Misawa and Nakamura, 1988; Pack et al., 2004; Patzer et al., 2018).

Fractionated ratios of RLEs in EC chondrules might indicate separation of sulfides from silicates and the depletion of nominally lithophile elements under highly reducing conditions (e.g., Ca, REE, Ti, Nb, Zr; Figs. 5 and B.4; Gannoun et al., 2011; Barrat et al., 2014; Lehner et al., 2014). The high Al/Ti and low Nb/Ta and Zr/Hf in EC chondrules are consistent with separation of Ti, Nb, Zr-bearing troilites from source materials having a CI composition. The sub-CI Ca/Al and REE/Al in EC chondrules reflect removal of oldhamite. The separation of oldhamites can also produce sub-CI Sm/Nd and negative Eu and Yb anomalies of EC chondrules (Fig. 2–4), given high Sm/Nd and positive Eu and Yb anomalies in oldhamites (Fig. B.4; Gannoun et al., 2011; Jacquet et al., 2015). Low Zr/Hf and Nb/Ta in EC chondrules (Fig. 2, 3) reflect the more lithophile behavior of Hf and Ta (Barrat et al., 2014; Münker et al., 2017). A CI-like Y/Ho value (~26; Pack et al., 2007; Barrat et al., 2012; Lodders, 2020) in EC chondrules (31.3 $\pm$ 6.7, $2\sigma_m$; Table A.3) document limited fractionation of this ratio by EC oldhamites. Stronger depletions of the troilite-loving elements (e.g., Ti, Nb) compared to the oldhamite-loving elements (e.g., REE, Y) in EC chondrules documents a greater contribution of troilite separation to their fractionated RLE compositions. This observation is consistent with a simple mass-balance for modal abundances of sulfides in type 3 EC (Weisberg and Kimura, 2012) and their average RLE concentrations (this study; Gannoun et al., 2011). Separation of RLE-bearing troilites from chondrule source materials produces >2 times larger RLE fractionation in residual silicates than the removal of oldhamite.

Chondrules from all types of chondrites are depleted in more normal siderophile and chalcophile elements because of the separation of metal and sulfide components from silicates before and/or during chondrule formation (Osborn et al., 1973; Gooding et al., 1980; Grossman et al., 1985; Palme et al., 2014). For example, metals and sulfides may

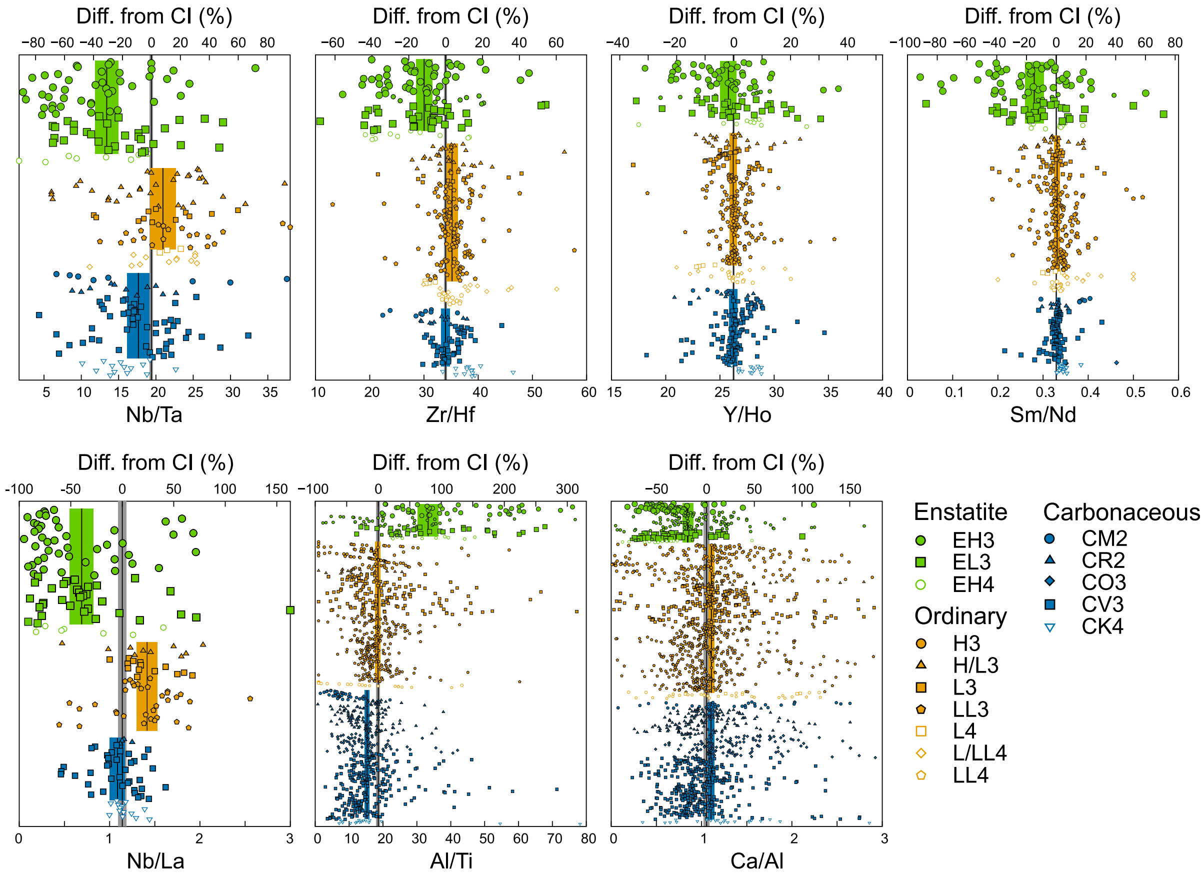

Fig. 4. Refractory lithophile element ratios (Nb/Ta, Zr/Hf, Y/Ho, Sm/Nd, Nb/La, Al/Ti, and Ca/Al) of bulk chondrules from unequilibrated type 3 enstatite (green), ordinary (orange) and carbonaceous (blue) chondrites. Our new data for type 3 EC chondrules are shown by large filled green circles (EH3) or squares (EL3). Colored boxes and inside solid lines represent mean $\pm 2\sigma_m$ values for each chondrite groups. Gray box and inside solid line correspond mean $\pm 2\sigma_m$ for CI chondrite (Barrat et al., 2012; Lodders, 2020). Data for chondrules from metamorphosed type 4 samples are also shown for a comparison. Most literature data are obtained from the ChondriteDB Database (Hezel et al., 2018b). A list of full data sources is provided as a supplementary material. (For interpretation of the references to color in this figure legend, the reader is referred to the web version of this article.)

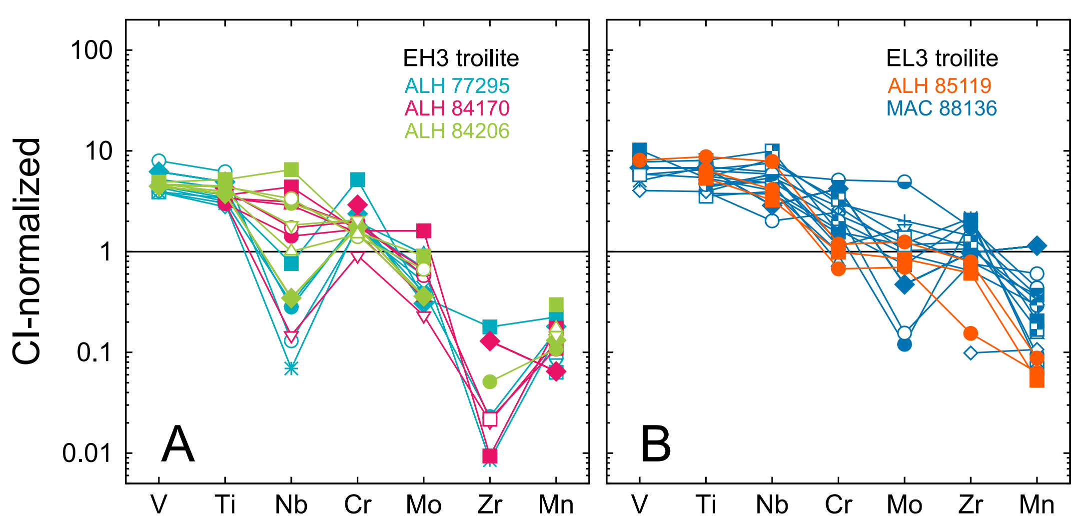

Fig. 5. Transition element composition of troilites (FeS) from unequilibrated EH and EL chondrite, normalized to CI chondrite composition (Lodders, 2020).

be expelled from silicate melt droplets during the chondrule formation as dense immiscible melts (Rambaldi and Wasson, 1981; Rambaldi and Wasson, 1984; Grossman and Wasson, 1985; Zanda et al., 1994; McCoy et al., 1999; Connolly et al., 2001; Uesugi et al., 2008). In addition, if metal/sulfide and silicate occurred separately in the protoplanetary disk as a result of the chondrule formation and/or nebular condensation, they could be physically sorted due to their distinct density, size, magnetism, and/or thermal conductivity (Kuebler et al., 1999; Wurm et al., 2013; Kruss and Wurm, 2020; Palme et al., 2014). These physical separation processes further enhance chemically-dependent fractionation processes.

The origin of metal-sulfide nodules in EC remains controversial. One view is that they are highly reduced nebular condensates formed and processed separately from silicates before planetesimal formation (Larimer, 1975; Larimer and Bartholomay, 1979; Larimer and Ganapathy, 1987; El Goresy et al., 1988; Kimura, 1988; Lin and El Goresy, 2002; Gannoun et al., 2011; El Goresy et al., 2017), whereas others propose that they were ejected from chondrule-forming melt droplets as immiscible liquids (Hsu, 1998; Horstmann et al., 2014; Lehner et al., 2014; Ebel et al., 2015; Jacquet et al., 2015; Piani et al., 2016) or combination of these processes (Lehner et al., 2010). The post-accretionary impact origin of these nodules is inconsistent with a lack of petrological and chemical features of in-situ melting (Horstmann et al., 2014; Gannoun et al., 2011; El Goresy et al., 2017).

The formation of metal-sulfide nodules and their separation from silicates can be critical processes in establishing Fe/Si ratio of bulk bodies with highly reduced oxidation states. The lower bulk Fe/Si value of EL chondrites as compared to EH (Fig. 1) can be partly attributed to less abundant occurrence of troilite in EL (<8 vol% and >10 vol% in primitive EL and EH, respectively; Weisberg and Kimura, 2012). The bulk EL composition should be depleted in moderately chalcophile RLE if low troilite abundances in EL reflect their ejection from chondrule-forming silicate melts. The same is true if there is limited troilite accretion on to EL parent bodies. However, neither bulk EH3 nor EL3 show fractionated RLE compositions (Barrat et al., 2014). Even ratios of RLE with different chalcophile affinities (e.g., Nb/La, Zr/Hf, Sc/Hf, Sc/Nb) are CI-like in the bulk EC (Barrat et al., 2014), which are distinct from highly fractionated RLE compositions of their chondrules (Fig. 2–4). These observations suggest that the depletion of moderately chalcophile RLE in EC silicates (i.e., chondrules) are complemented by RLE-bearing sulfides in the bulk EC, and removal of sulfides from chondrule-forming melts did not contribute to the low troilite abundance in EL. Thus, metal- and sulfide-depletions in EC chondrules and CI-like RLE ratios found in bulk EC document that EC silicates and metal-sulfide nodules occurred as separate objects in the protoplanetary disk, but none of them were preferentially removed from the local source material before and during the EC parent body accretion. Limited physical sorting of EC silicates, sulfides, and metals requires that separation was a localized process in the protoplanetary disk and EC parent bodies accreted quickly after chondrule forming events. The fractionated RLE ratios of EC components (Fig. 4) and solar-like RLE ratio of the bulk EC (Barrat et al., 2014) might support a compositional complementarity between chondrules and other components (e.g., Hezel et al., 2018a).

Constraining the timing and mechanism of RLE fractionation recorded by EC chondrules and sulfides, especially those in EH, demands an understanding of the redox-dependent changes of RLE volatilities. Although multiple equilibrium condensation calculations have been performed for highly reducing conditions (e.g., Larimer, 1975; Larimer and Bartholomay, 1979; Lodders and Fegley, 1993; Wood and Hashimoto, 1993; Sharp and Wasserburg, 1995; Ebel, 2006; Ebel and Alexander, 2011), relative volatilities of minor and trace RLE, especially those for troilite-loving ones (e.g., Ti, Nb), are poorly understood. A combination of relative volatilities and chalcophile affinities of RLE under reducing conditions will provide important constraints on the RLE fractionation mechanism prior to the accretion of EC parent bodies.

4.2. Compositional difference between EC chondrules and the silicate Earth

The limited variation (<10%) in RLE ratios among chondritic meteorites and the solar photosphere have led planetary scientists to use the constant RLE ratio rule in their compositional models of planets (Section 1). In contrast, the fractionated RLE ratios of EC chondrules (Figs. 2 to 4) potentially places limits on the use of this rule, when modeling composition of highly reduced bodies (e.g., Mercury; Section 4.4). In turn, these variations can be used as a new key to reveal the nature of planetary building blocks, together with the isotopic constraints (e.g., Javoy et al., 2010; Warren, 2011; Dauphas, 2017).

Isotopic similarities of Earth and EC suggest EC-like materials as the Earth's main building block (e.g., Javoy et al., 2010; Warren, 2011; Dauphas, 2017; Boyet et al., 2018). In this case, the Earth's mantle could have been dominated by EC chondrule-like materials, as they host nearly all of silicates in EC (e.g., Weisberg and Kimura, 2012; Krot et al., 2014). EC chondrules and the Earth's mantle share Nb depletions, with Nb/Ta and Nb/La values being 20–30% lower than the CI chondritic values (Fig. 4; Münker et al., 2003). In contrast, composition of terrestrial komatiites, high-temperature ultramafic rocks mostly formed in the Archean, is consistent with a CI-like Ti/RLE values for the Earth's primitive mantle, and thus there is no Ti depletion in the BSE (e.g., Nesbitt et al., 1979; McDonough and Sun, 1995; Arndt, 2003). Fractionated, non-CI-like Al/Ti values of EC chondrules highlight their compositional difference with the BSE.

Experimental studies show that Nb and Ti have similar $D^{\mathrm{sulfide/silicate}}$ values at wide P, T, and f_{O_2} conditions, with the value exceeding 1 at highly reduced conditions ($\log f_{O_2} \leqslant \mathrm{IW} - 2$; Fig. 6A; Kiseeva and Wood, 2015; Wood and Kiseeva, 2015; Namur et al., 2016; Münker et al., 2017; Cartier et al., 2020; Steenstra and van Westrenen, 2020). Compositions of troilites and silicates from aubrites, highly reduced achondrites, find similar

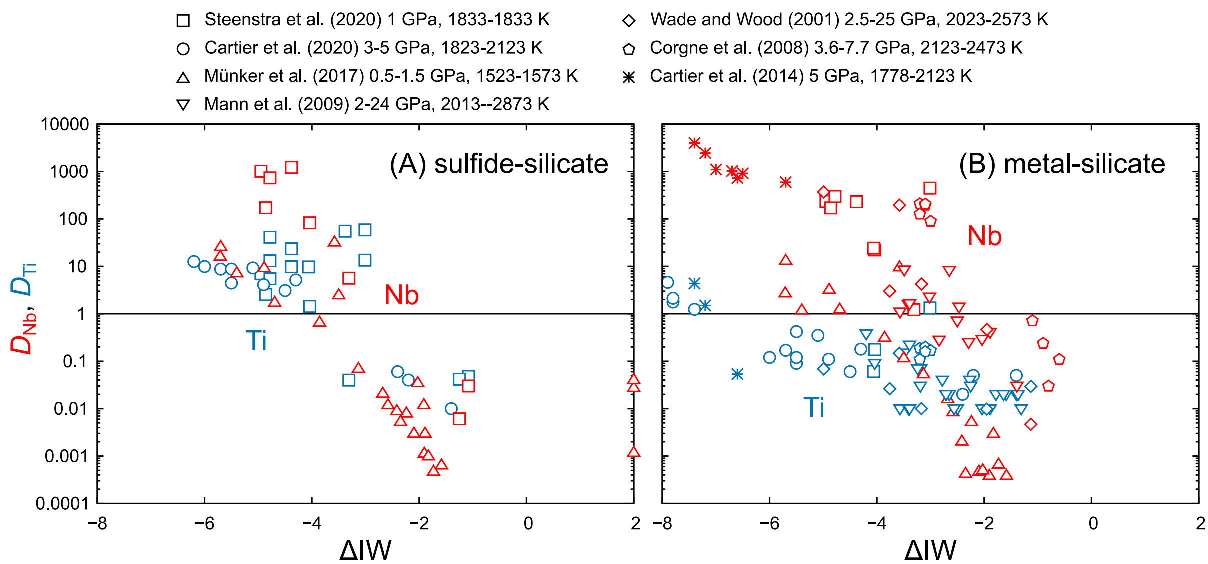

Fig. 6. (A) Sulfide-silicate and (B) metal-silicate partition coefficients of Nb (blue) and Ti (red) reported by previous studies (Wade and Wood, 2001; Corgne et al., 2008; Mann et al., 2009; Cartier et al., 2014, 2020; Münker et al., 2017; Steenstra and van Westrenen, 2020). (For interpretation of the references to color in this figure legend, the reader is referred to the web version of this article.)

chalcophile behavior of Nb and Ti during differentiation of aubrite parent bodies (van Acken et al., 2012; Münker et al., 2017). Thus, sulfide-silicate fractionation under highly reduced conditions produces not only Nb, but also Ti depletion in silicates at a similar degree. However, Ti is not depleted in the BSE (e.g., Nesbitt et al., 1979; McDonough and Sun, 1995; Arndt, 2003). Therefore, even if the EC chondrules are the Earth's main building block (Javoy et al., 2010; Warren, 2011; Dauphas, 2017; Boyet et al., 2018), the apparent accessible Earth's Nb depletion should not have resulted from a sulfide-silicate separation under highly reduced conditions. There is negligible evidence for core forming extraction of a highly reduced sulfide in the BSE composition (e.g., McDonough and Sun, 1995; Pack et al., 2007; Bouvier et al., 2008; Bouvier and Boyet, 2016; Burkhardt et al., 2016; Willig et al., 2020) (cf. Stracke et al., 2012; Dauphas and Pourmand, 2015) and a lack of evidence for Th and U incorporation into the Earth's core (Wipperfurth et al., 2018).

Experimental studies show that Nb becomes siderophile under reducing conditions ($\log f_{O_2} \leqslant IW - 2$), whereas Ti remains lithophile (Fig. 6B; Wade and Wood, 2001; Corgne et al., 2008; Mann et al., 2009; Namur et al., 2016; Cartier et al., 2020; Steenstra and van Westrenen, 2020). Thus, metal-silicate differentiation under reduced conditions can selectively separates Nb from silicate melts, leaving Ti as oxide in the mantle. Therefore, the siderophile behavior of Nb under reduced conditions might be a most plausible scenario for the origin of the BSE's apparent Nb depletion (Wade and Wood, 2001; Münker et al., 2003). Recently, Münker et al. (2017) experimentally showed that Nb becomes less chalcophile when Fe/S of a sulfide melt increases. Thus, it is likely that the siderophile behavior of Nb in the Earth reflects the low S content of the Earth's core (Dreibus and Palme, 1996; McDonough, 2014).

4.3. The Earth's building blocks

Fractionated RLE ratios in EC components provide insights into the nature of the Earth's building blocks, which may be dominated by EC-like materials based on isotopic constraints (e.g., Javoy et al., 2010; Warren, 2011; Dauphas, 2017; Boyet et al., 2018). Multiple observations document that the BSE has CI-like RLE ratios (e.g., Al/Ti, Zr/Hf, Ca/Al and Sm/Nd, excepting possibly Nb/RLE; Bouvier et al., 2008; Bouvier and Boyet, 2016; Burkhardt et al., 2016; Hasenstab et al., 2020; McDonough and Sun, 1995; Münker et al., 2003; Stracke et al., 2012; Willig and Stracke, 2019). If the Earth's accretion was dominated by highly reduced, EC-like materials, their silicate fraction might have fractionated RLE ratios due to depletion of nominally lithophile, but moderately chalcophile refractory elements (e.g., Ti, Zr, Ca, REE), as we have observed in EC chondrules (Figs. 2–4). To produce the CI-like RLE ratios of the BSE, the reduced silicates and RLE-bearing sulfides should have been jointly incorporated into the accreting Earth. Subsequently, RLE hosted in these sulfides from the impactors must have been re-incorporated into the silicate mantle, which is consistent with a progressive oxidation of the Earth's interior (Corgne et al., 2008; Mann et al., 2009; Schönbächler et al., 2010; Rubie et al., 2011; Rubie et al., 2015). An important implication of this scenario is that the Earth's silicates and sulfides should have originated in the same chemical reservoir of solar-like composition. In addition, these silicates and sulfides should have accreted to planetesimals before being physically separated in the protoplanetary disk.

Alternatively, the distinct RLE composition of silicate fractions of EC and Earth might reflect distinct formation temperatures of their precursors. Importantly, the bulk Earth is depleted in S and has a chondritic Fe/Si (Dreibus and Palme, 1996; McDonough, 2014), which require that the S depletion was established during nebular condensation, rather than physical sulfide-silicate separation. Under highly reducing nebular conditions as recorded by EC, refractory sulfides such as oldhamite and niningerite condense at 1000–800 K, whereas troilite condenses at <700 K as a major S-bearing phase (Hutson and Ruzicka, 2000; Pasek et al., 2005). Therefore, RLE compositions of highly reduced silicates condensed before the condensation of these sulfides should not have been fractionated due to sulfide-silicate separation as recorded in EC chondrules. This scenario supports the condensation of Earth's precursors at higher temperatures compared to EC materials. Lower temperature condensation of EC materials has been proposed, based on their elevated abundances of moderately volatile elements and low Mg/Si and RLE/Mg ratios (Kerridge, 1979; Larimer, 1979; Dauphas et al., 2015; Morbidelli et al., 2020; Yoshizaki and McDonough, in press).

Our observations revealed distinct RLE compositions of the silicate fractions of EC and Earth, which further emphasize their compositional distinctions between EC and Earth (Palme et al., 1988; McDonough and Sun, 1995; Yoshizaki and McDonough, in press). These distinctions reflect an unrepresentative sampling of the solar system materials in our meteorite collections (DeMeo and Carry, 2014; Heck et al., 2017) and/or a lack of leftovers of the Earth's building blocks in the present-day solar system (Drake and Righter, 2002). Although there is no meteorite group that matches the chemical and isotopic composition of Earth, EC and their components provide unique and useful guides to the origin, nature, and geochemical evolution of the Earth-forming materials (Dauphas et al., 2015; Morbidelli et al., 2020; Yoshizaki and McDonough, in press).

4.4. Implications for the composition of Mercury

The RLE fractionation observed in the silicate fraction of EC (Fig. 2–4) indicates that caution is needed when modeling RLE abundance of highly reduced bodies that have experienced an open-system metal-silicate separation (e.g., physical sorting before and during planetary accretion, collisional erosion of a mantle). The most notable example is Mercury, which is one of the most reduced bodies in our solar system and has an elevated bulk Fe/Si ratio that might reflect a selective removal of silicates and/or preferred accretion of metal/sulfide phases (Nittler et al., 2011; Ebel and Stewart, 2018; Margot et al., 2018; McDonough and Yoshizaki, in press).

The elemental abundance of the Mercury's surface was measured by the MErcury Surface, Space ENvironment, GEochemistry, and Ranging (MESSENGER) spacecraft, which provided important constraints on the chemical composition and interior structure of the planet (Nittler et al., 2011; Nittler et al., 2018; Nittler et al., 2020; Peplowski et al., 2011). Recently, Cartier et al. (2020) showed that Al/Ti ratio in the bulk silicate Mercury is ~50% higher than the CI value, based on the MESSENGER data. By assuming that the bulk Mercury has a chondritic Al/Ti value, the authors concluded that the Ti depletion in the Mercury's surface was produced by a S-bearing core formation under reducing condition, and estimated a thickness of a troilite layer at the core-mantle boundary. In contrast, chondrules and sulfides from EC show clear evidence for Al/Ti fractionation in a highly reduced nebular environment before planetary accretion and differentiation (Fig. 4). Therefore, the super-CI Al/Ti value of the Mercury's silicate shell might reflect both nebular and planetary RLE fractionation processes under reducing conditions. Importantly, if the planet preferentially accreted metal/sulfide phases (Wurm et al., 2013; Kruss and Wurm, 2018; Kruss and Wurm, 2020), bulk Mercury can be enriched in moderately chalcophile RLE (e.g., Ti, REE, Nb, Ca) compared to Al, thereby invalidating the constant RLE ratio rule. Thus, the constant RLE rule should be used with caution, at least when estimating chemical compositions of highly reduced bodies.

As we described in Section 4.3, highly reduced silicates condensing from a cooling nebular gas before the condensation of RLE-bearing sulfides may not be affected by a significant RLE fractionation due to sulfide-silicate separation. The observations from the MESSENGER mission indicate that the surface materials of Mercury have less fractionated RLE ratios and lower abundances of moderately volatile elements as compared to the silicate fractions of EC (Nittler et al., 2011; Nittler et al., 2018; Nittler et al., 2020; Peplowski et al., 2011; Evans et al., 2015; Cartier et al., 2020). These observations allow for the possibility that the building blocks of Mercury condensed at higher temperatures than EC materials (i.e., before sulfide condensation), as we proposed for the Earth's precursor materials.

5. CONCLUSIONS

Refractory lithophile elements (RLE) can be fractionated due to their different chalcophile affinities under highly reducing nebular conditions. Chondrules from enstatite chondrites (EC) record RLE fractionation due to a sulfide-silicate separation before and/or during chondrule formation events under a highly reduced nebular environments, documenting that RLE ratios can be variable among silicates in the planetary building blocks. In contrast, bulk EC have CI-like RLE ratios, indicating a negligible physical sorting of silicates and sulfides before and during the accretion of EC parent bodies. Similarly, the Earth's building blocks might have not experienced the physical sorting of silicates and sulfides. Alternatively, they have condensed from a high-temperature nebular gas in which RLE-bearing sulfides were not stable. The accessible Earth's apparent Nb depletion and its chondritic Ti/RLE values might reflect the moderately siderophile behavior of Nb during the Earth's accretion. The moderately chalcophile behavior of RLE under highly reducing conditions indicate that the bulk Mercury cannot yield CI-like RLE ratios if its large core/mantle ratio is originated in a selective removal of silicates.

CREDIT AUTHORSHIP CONTRIBUTION STATEMENT

Takashi Yoshizaki: Conceptualization, Methodology, Validation, Formal analysis, Investigation, Resources,

Data curation, Writing - original draft, Visualization, Project administration, Funding acquisition. **Richard D. Ash:** Methodology, Validation, Formal analysis, Investigation, Writing - review & editing. **Marc D. Lipella:** Formal analysis, Investigation, Data curation. **Tetsuya Yokoyama:** Writing - review & editing, Funding acquisition. **William F. McDonough:** Conceptualization, Methodology, Validation, Formal analysis, Writing - review & editing, Funding acquisition.

Declaration of Competing Interest

The authors declare that they have no known competing financial interests or personal relationships that could have appeared to influence the work reported in this paper.

ACKNOWLEDGMENTS

We thank Roberta Rudnick and Philip Piccoli for discussions and technical assistance, Issei Narita for technical assistance, Dominik Hezel for kindly providing the ChondriteDB spreadsheet. We appreciate Conel Alexander and Kevin Righter for their helpful comments. We greatly appreciate Herbert Palme, Andreas Stracke, Dominik Hezel, and an anonymous referee for their constructive reviews, which helped improve the manuscript. We thank the associate editor Stefan Weyer for his editorial effort. We are grateful to NASA/JSC for loan of ALH 84170, ALH 84206, ALH 85119, MAC 88136 and RBT 04143, National Institute of Polar Research for ALHA77295, and the Smithsonian Institute for Allende. This work was supported by Grant-in-Aid for JSPS Research Fellow (No. JP18J20708), GP-EES Research Grant and DIARE Research Grant to TaY, JSPS KAKENHI Grant (No. 16H04081) to TeY, and NSF grant EAR1650365 to WFM.

APPENDIX A. SUPPLEMENTARY MATERIAL

Supplementary data associated with this article can be found, in the online version, at https://doi.org/10.1016/j.gca.2021.05.057.

REFERENCES

van Achterbergh E., Ryan C. G., Jackson S. E. and Griffin W. L. (2001) Appendix 3: Data reduction software for LA-ICP-MS. In *Laser Ablation-ICP-MS in the Earth Sciences: Principles and Applications. Mineralogical Association of Canada, Québec. Mineralogical Association of Canada-Short Course Series*, vol. 29 (ed. P. Sylvester), pp. 239–243.

van Acken D., Humayun M., Brandon A. D. and Peslier A. H. (2012) Siderophile trace elements in metals and sulfides in enstatite achondrites record planetary differentiation in an enstatite chondritic parent body. *Geochim. Cosmochim. Acta* **83**, 272–291.

Alexander C. M. O'D. (2005) Re-examining the role of chondrules in producing the elemental fractionations in chondrites. *Meteor. Planet. Sci.* **40**, 943–965.

Alexander C. M. O'D. (2019a) Quantitative models for the elemental and isotopic fractionations in chondrites: The carbonaceous chondrites. *Geochim. Cosmochim. Acta* **254**, 277–309.

Alexander C. M. O'D. (2019b) Quantitative models for the elemental and isotopic fractionations in the chondrites: The non-carbonaceous chondrites. *Geochim. Cosmochim. Acta* **254**, 246–276.

Allègre C. J., Poirier J. P., Humler E. and Hofmann A. W. (1995) The chemical composition of the Earth. *Earth Planet. Sci. Lett.* **134**, 515–526.

Amsellem E., Moynier F., Pringle E. A., Bouvier A., Chen H. and Day J. M. D. (2017) Testing the chondrule-rich accretion model for planetary embryos using calcium isotopes. *Earth Planet. Sci. Lett.* **469**, 75–83.

Arndt N. T. (2003) Komatiites, kimberlites, and boninites. *J. Geophys. Res. Solid Earth* **108**, 2293.

Barrat J. A., Dauphas N., Gillet P., Bollinger C., Etoubleau J., Bischoff A. and Yamaguchi A. (2016) Evidence from Tm anomalies for non-CI refractory lithophile element proportions in terrestrial planets and achondrites. *Geochim. Cosmochim. Acta* **176**, 1–17.

Barrat J. A., Zanda B., Jambon A. and Bollinger C. (2014) The lithophile trace elements in enstatite chondrites. *Geochim. Cosmochim. Acta* **128**, 71–94.

Barrat J. A., Zanda B., Moynier F., Bollinger C., Liorzou C. and Bayon G. (2012) Geochemistry of CI chondrites: Major and trace elements, and Cu and Zn isotopes. *Geochim. Cosmochim. Acta* **83**, 79–92.

Benoit P. H., Akridge G. A., Ninagawa K. and Sears D. W. G. (2002) Thermoluminescence sensitivity and thermal history of type 3 ordinary chondrites: Eleven new type 3.0–3.1 chondrites and possible explanations for differences among H, L, and LL chondrites. *Meteor. Planet. Sci.* **37**, 793–805.

Bonal L., Gattacceca J., Garenne A., Eschrig J., Rochette P. and Ruggiu L. K. (2020) Water and heat: New constraints on the evolution of the CV chondrite parent body. *Geochim. Cosmochim. Acta* **276**, 363–383.

Bouvier A. and Boyet M. (2016) Primitive Solar System materials and Earth share a common initial ^{142}Nd abundance. *Nature* **537**, 399–402.

Bouvier A., Vervoort J. D. and Patchett P. J. (2008) The Lu–Hf and Sm–Nd isotopic composition of CHUR: Constraints from unequilibrated chondrites and implications for the bulk composition of terrestrial planets. *Earth Planet. Sci. Lett.* **273**, 48–57.

Boyet M., Bouvier A., Frossard P., Hammouda T., Garçon M. and Gannoun A. (2018) Enstatite chondrites EL3 as building blocks for the Earth: The debate over the ^{146}Sm–^{142}Nd systematics. *Earth Planet. Sci. Lett.* **488**, 68–78.

Boynton W. V. (1975) Fractionation in the solar nebula: Condensation of yttrium and the rare earth elements. *Geochim. Cosmochim. Acta* **39**, 569–584.

Braukmüller N., Wombacher F., Hezel D. C., Escoube R. and Münker C. (2018) The chemical composition of carbonaceous chondrites: Implications for volatile element depletion, complementarity and alteration. *Geochim. Cosmochim. Acta* **239**, 17–48.

Burkhardt C., Borg L. E., Brennecka G. A., Shollenberger Q. R., Dauphas N. and Kleine T. (2016) A nucleosynthetic origin for the Earth's anomalous ^{142}Nd composition. *Nature* **537**, 394–398.

Cartier C., Hammouda T., Boyet M., Bouhifd M. A. and Devidal J. L. (2014) Redox control of the fractionation of niobium and tantalum during planetary accretion and core formation. *Nat. Geosci.* **7**, 573–576.

Cartier C., Namur O., Nittler L. R., Weider S. Z., Crapster-Pregont E., Vorburger A., Franck E. A. and Charlier B. (2020) No FeS layer in Mercury? Evidence from Ti/Al measured by MESSENGER. *Earth Planet. Sci. Lett.* **534**, 116108.

Clayton R. N. (2003) Oxygen isotopes in meteorites. In *Meteorites, Comets, and Planets. Treatise on Geochemistry*, vol. 1 (eds. H.

D. Holland and K. K. Turekian). Elsevier, Oxford, pp. 129–142.

Connolly, Jr., H. C., Huss G. R. and Wasserburg G. J. (2001) On the formation of Fe-Ni metal in Renazzo-like carbonaceous chondrites. *Geochim. Cosmochim. Acta* **65**, 4567–4588.

Corgne A., Keshav S., Wood B. J., McDonough W. F. and Fei Y. (2008) Metal–silicate partitioning and constraints on core composition and oxygen fugacity during Earth accretion. *Geochim. Cosmochim. Acta* **72**, 574–589.

Dauphas N. (2017) The isotopic nature of the Earth's accreting material through time. *Nature* **541**, 521–524.

Dauphas N., Poitrasson F., Burkhardt C., Kobayashi H. and Kurosawa K. (2015) Planetary and meteoritic Mg/Si and δ^{30}Si variations inherited from solar nebula chemistry. *Earth Planet. Sci. Lett.* **427**, 236–248.

Dauphas N. and Pourmand A. (2015) Thulium anomalies and rare earth element patterns in meteorites and Earth: Nebular fractionation and the nugget effect. *Geochim. Cosmochim. Acta* **163**, 234–261.

DeMeo F. E. and Carry B. (2014) Solar System evolution from compositional mapping of the asteroid belt. *Nature* **505**, 629–634.

Drake M. J. and Righter K. (2002) Determining the composition of the Earth. *Nature* **416**, 39–44.

Dreibus G. and Palme H. (1996) Cosmochemical constraints on the sulfur content in the Earth's core. *Geochim. Cosmochim. Acta* **60**, 1125–1130.

Ebel D. S. (2006) Condensation of rocky material in astrophysical environments. In *Meteorites and the Early Solar System II* (eds. D. S. Lauretta and , Jr.H. Y. McSween). The University of Arizona Press, Tucson, pp. 253–277.

Ebel D. S. and Alexander C. M. O'D. (2011) Equilibrium condensation from chondritic porous IDP enriched vapor: Implications for Mercury and enstatite chondrite origins. *Planet. Space Sci.* **59**, 1888–1894.

Ebel D. S., Boyet M., Hammouda T., Gannoun A., Weisberg M. K. and El Goresy A. (2015) Complementary rare Earth element abundances in enstatite and oldhamite in EH3 chondrites. In *Lunar and Planetary Science Conference*, p. 2619.

Ebel D. S. and Stewart S. T. (2018) The elusive origin of Mercury. In *Mercury: The View after MESSENGER* (eds. S. C. Solomon, L. R. Nittler and B. J. Anderson). Cambridge University Press, Cambridge, pp. 497–515.

El Goresy A., Lin Y., Miyahara M., Gannoun A., Boyet M., Ohtani E., Gillet P., Trieloff M., Simionovici A., Feng L. and Lemelle L. (2017) Origin of EL3 chondrites: Evidence for variable C/O ratios during their course of formation–A state of the art scrutiny. *Meteor. Planet. Sci.* **52**, 781–806.

El Goresy A., Yabuki H., Ehlers K., Woolum D. and Pernicka E. (1988) Qingzhen and Yamato-691: A tentative alphabet for the EH chondrites. *Antarct. Meteor. Res.* **1**, 65–101.

El Goresy A., Zinner E., Matsunami S., Palme H., Spettel B., Lin Y. and Nazarov M. (2002) Efremovka 101.1: A CAI with ultrarefractory REE patterns and enormous enrichments of Sc, Zr, and Y in fassaite and perovskite. *Geochim. Cosmochim. Acta* **66**, 1459–1491.

Evans L. G., Peplowski P. N., McCubbin F. M., McCoy T. J., Nittler L. R., Zolotov M. Y., Ebel D. S., Lawrence D. J., Starr R. D., Weider S. Z. and Solomon S. C. (2015) Chlorine on the surface of Mercury: MESSENGER gamma-ray measurements and implications for the planet's formation and evolution. *Icarus* **257**, 417–427.

Gannoun A., Boyet M., El Goresy A. and Devouard B. (2011) REE and actinide microdistribution in Sahara 97072 and ALHA77295 EH3 chondrites: A combined cosmochemical and petrologic investigation. *Geochim. Cosmochim. Acta* **75**, 3269–3289.

Gerber M. (2012) *Chondrule formation in the early Solar System: A combined ICP-MS, ICP-OES and petrological study* (Ph.D. thesis). University of Münster.

Gooding J. L., Keil K., Fukuoka T. and Schmitt R. A. (1980) Elemental abundances in chondrules from unequilibrated chondrites: Evidence for chondrule origin by melting of pre-existing materials. *Earth Planet. Sci. Lett.* **50**, 171–180.

Grossman J. N. and Brearley A. J. (2005) The onset of metamorphism in ordinary and carbonaceous chondrites. *Meteor. Planet. Sci.* **40**, 87–122.

Grossman J. N., Rubin A. E., Rambaldi E. R., Rajan R. S. and Wasson J. T. (1985) Chondrules in the Qingzhen type-3 enstatite chondrite: Possible precursor components and comparison to ordinary chondrite chondrules. *Geochim. Cosmochim. Acta* **49**, 1781–1795.

Grossman J. N. and Wasson J. T. (1985) The origin and history of the metal and sulfide components of chondrules. *Geochim. Cosmochim. Acta* **49**, 925–939.

Hasenstab E., Tusch J., Schnabel C., Marien C. S., Van Kranendonk M. J., Smithies H., Howard H., Maier W. D. and Münker C. (2020) Evolution of the early to late Archean mantle from Hf-Nd-Ce isotope systematics in basalts and komatiites from the Pilbara Craton. *Earth Planet. Sci. Lett.* **553**, 116627.

Heck P. R., Schmitz B., Bottke W. F., Rout S. S., Kita N. T., Cronholm A., Defouilloy C., Dronov A. and Terfelt F. (2017) Rare meteorites common in the Ordovician period. *Nat. Astron.* **1**, 0035.

Hewins R. H. and Herzberg C. T. (1996) Nebular turbulence, chondrule formation, and the composition of the Earth. *Earth Planet. Sci. Lett.* **144**, 1–7.

Hezel D. C., Bland P., Palme H., Jacquet E. and Bigolski J. (2018a) Composition of chondrules and matrix and their complementary relationship in chondrites. In *Chondrules and the Protoplanetary Disk* (eds. S. S. Russell, , Jr.H. C. Connolly and A. N. Krot). Cambridge University Press, Cambridge, pp. 91–121 (Chapter 4).

Hezel D. C., Harak M. and Libourel G. (2018b) What we know about elemental bulk chondrule and matrix compositions: Presenting the ChondriteDB Database. *Chemie der Erde-Geochemistry* **78**, 1–14.

Hezel D. C. and Parteli E. J. (2018) The spatial origin of chondrules in individual chondrites: Constraints from modeling chondrule mixing. *Astrophys. J.* **863**, 54.

Horstmann M., Humayun M. and Bischoff A. (2014) Clues to the origin of metal in Almahata Sitta EL and EH chondrites and implications for primitive E chondrite thermal histories. *Geochim. Cosmochim. Acta* **140**, 720–744.

Hsu W. (1998) Geochemical and petrographic studies of oldhamite, diopside, and roedderite in enstatite meteorites. *Meteor. Planet. Sci.* **33**, 291–301.

Hutson M. and Ruzicka A. (2000) A multi-step model for the origin of E3 (enstatite) chondrites. *Meteori. Planet. Sci.* **35**, 601–608.

Ishida H., Nakamura T., Miura H. and Kakazu Y. (2012) Diverse mineralogical and oxygen isotopic signatures recorded in CV3 carbonaceous chondrites. *Polar Sci.* **6**, 252–262.

Jacquet E., Alard O. and Gounelle M. (2015) The formation conditions of enstatite chondrites: Insights from trace element geochemistry of olivine-bearing chondrules in Sahara 97096 (EH3). *Meteor. Planet. Sci.* **50**, 1624–1642.

Jacquet E., Piani L. and Weisberg M. K. (2018) Chondrules in enstatite chondrites. In *Chondrules: Records of Protoplanetary Disk Processes*, vol. 22 (eds. S. S. Russell, , Jr.H. C. Connolly and A. N. Krot). Cambridge University Press, Cambridge, pp. 175–195 (chapter 7).

Javoy M., Kaminski E., Guyot F., Andrault D., Sanloup C., Moreira M., Labrosse S., Jambon A., Agrinier P., Davaille A. and Jaupart C. (2010) The chemical composition of the Earth: Enstatite chondrite models. *Earth Planet. Sci. Lett.* **293**, 259–268.

Jochum K. P. and Nohl U. (2008) Reference materials in geochemistry and environmental research and the GeoReM database. *Chem. Geol.* **253**, 50–53.

Jochum K. P., Weis U., Stoll B., Kuzmin D., Yang Q., Raczek I., Jacob D. E., Stracke A., Birbaum K., Frick D. A., Günther D. and Enzweiler J. (2011) Determination of reference values for NIST SRM 610–617 glasses following ISO guidelines. *Geostand. Geoanal. Res.* **35**, 397–429.

Johansen A., Mac Low M. M., Lacerda P. and Bizzarro M. (2015) Growth of asteroids, planetary embryos, and Kuiper belt objects by chondrule accretion. *Sci. Adv.* **1**, e1500109.

Johnson T. and Lofgren G. E. (1995) Relative abundances of chondrule textural types in E3 chondrites. In *Lunar and Planetary Science Conference*, pp. 689–690.

Jones R. H. (2012) Petrographic constraints on the diversity of chondrule reservoirs in the protoplanetary disk. *Meteor. Planet. Sci.* **47**, 1176–1190.

Kamber B. S. and Collerson K. D. (2000) Role of 'hidden' deeply subducted slabs in mantle depletion. *Chem. Geol.* **166**, 241–254.

Keil K. (1968) Mineralogical and chemical relationships among enstatite chondrites. *J. Geophys. Res.* **73**, 6945–6976.

Kerridge J. (1979) Fractionation of refractory lithophile elements among chondritic meteorites. In *Lunar and Planetary Science Conference Proceedings*, pp. 989–996.

Kimura M. (1988) Origin of opaque minerals in an unequilibrated enstatite chondrite, Yamato-691. *Antarct. Meteor. Res.* **1**, 51–64.

Kiseeva E. S. and Wood B. J. (2015) The effects of composition and temperature on chalcophile and lithophile element partitioning into magmatic sulphides. *Earth Planet. Sci. Lett.* **424**, 280–294.

Kornacki A. S. and Fegley, Jr., B. (1986) The abundance and relative volatility of refractory trace elements in Allende Ca, Al-rich inclusions: Implications for chemical and physical processes in the solar nebula. *Earth Planet. Sci. Lett.* **79**, 217–234.

Krot A. N., Nagashima K. and Petaev M. I. (2012) Isotopically uniform, ^{16}O-depleted calcium, aluminum-rich inclusions in CH and CB carbonaceous chondrites. *Geochim. Cosmochim. Acta* **83**, 159–178.

Krot A. N., Scott E. R. D., Goodrich C. A. and Weisberg M. K. (2014) Chondrites and their Components. In *Treatise on Geochemistry (second ed.)*, vol. 1 (eds. H. D. Holland and K. K. Turekian). Elsevier, Oxford, pp. 1–63.

Kruss M. and Wurm G. (2018) Seeding the Formation of Mercurys: An Iron-sensitive Bouncing Barrier in Disk Magnetic Fields. *Astrophys. J.* **869**, 45.

Kruss M. and Wurm G. (2020) Composition and size dependent sorting in preplanetary growth: seeding the formation of Mercury-like planets. *Planet. Sci. J.* **1**, 23.

Kuebler K. E., McSween, Jr., H. Y., Carlson W. D. and Hirsch D. (1999) Sizes and masses of chondrules and metal–troilite grains in ordinary chondrites: Possible implications for nebular sorting. *Icarus* **141**, 96–106.

Larimer J. W. (1968) An experimental investigation of oldhamite, CaS; and the petrologic significance of oldhamite in meteorites. *Geochim. Cosmochim. Acta* **32**, 965–982.

Larimer J. W. (1975) The effect of C/O ratio on the condensation of planetary material. *Geochim. Cosmochim. Acta* **39**, 389–392.

Larimer J. W. (1979) The condensation and fractionation of refractory lithophile elements. *Icarus* **40**, 446–454.

Larimer J. W. and Bartholomay M. (1979) The role of carbon and oxygen in cosmic gases: Some applications to the chemistry and mineralogy of enstatite chondrites. *Geochim. Cosmochim. Acta* **43**, 1455–1466.

Larimer J. W. and Ganapathy R. (1987) The trace element chemistry of CaS in enstatite chondrites and some implications regarding its origin. *Earth Planet. Sci. Lett.* **84**, 123–134.

Larimer J. W. and Wasson J. T. (1988) Refractory lithophile elements. In *Meteorites and the Early Solar System* (eds. J. F. Kerridge and M. S. Matthews). University of Arizona Press, Tucson, pp. 394–415.

Lehner S. W., Buseck P. R. and McDonough W. F. (2010) Origin of kamacite, schreibersite, and perryite in metal-sulfide nodules of the enstatite chondrite Sahara 97072 (EH3). *Meteor. Planet. Sci.* **45**, 289–303.

Lehner S. W., McDonough W. F. and Németh P. (2014) EH3 matrix mineralogy with major and trace element composition compared to chondrules. *Meteor. Planet. Sci.* **49**, 2219–2240.

Levison H. F., Kretke K. A., Walsh K. J. and Bottke W. F. (2015) Growing the terrestrial planets from the gradual accumulation of submeter-sized objects. *Proc. Nat. Acad. Sci.* **112**, 14180–14185.

Lin Y. and El Goresy A. (2002) A comparative study of opaque phases in Qingzhen (EH3) and MacAlpine Hills 88136 (EL3): Representatives of EH and EL parent bodies. *Meteor. Planet. Sci.* **37**, 577–599.

Lodders K. (2003) Solar system abundances and condensation temperatures of the elements. *Astrophys. J.* **591**, 1220–1247.

Lodders K. (2020) Solar Elemental Abundances. In *Oxford Research Encyclopedia of Planetary Science* (ed. P. Read). Oxford University Press, Oxford, pp. 1–68.

Lodders K. and Fegley, Jr., B. (1993) Lanthanide and actinide chemistry at high C/O ratios in the solar nebula. *Earth Planet. Sci. Lett.* **117**, 125–145.

Mann U., Frost D. J. and Rubie D. C. (2009) Evidence for high-pressure core-mantle differentiation from the metal–silicate partitioning of lithophile and weakly-siderophile elements. *Geochim. Cosmochim. Acta* **73**, 7360–7386.

Margot J. L., Hauck I., Steven A., Mazarico E., Padovan S. and Peale S. J. (2018) Mercury's internal structure. In *Mercury: The View after MESSENGER* (eds. S. C. Solomon, L. R. Nittler and B. J. Anderson). Cambridge University Press, Cambridge, pp. 85–113.

Mason B. and Martin P. M. (1977) Geochemical differences among components of the Allende meteorite. *Smithson. Contrib. Earth Sci.* **19**, 84–95.

McCoy T. J., Dickinson T. L. and Lofgren G. E. (1999) Partial melting of the Indarch (EH4) meteorite: A textural, chemical, and phase relations view of melting and melt migration. *Meteor. Planet. Sci.* **34**, 735–746.

McDonough W. F. (1991) Partial melting of subducted oceanic crust and isolation of its residual eclogitic lithology. *Philos. Trans. Roy. Soc. Lond. Math. Phys. Eng. Sci.* **335**, 407–418.

McDonough W. F. (2014) Compositional model for the Earth's core. In *Treatise on Geochemistry (second ed.)*, vol. 3 (eds. H. D. Holland and K. K. Turekian). Elsevier, Oxford, pp. 559–577.

McDonough W. F. and Sun S. S. (1995) The composition of the Earth. *Chem. Geol.* **120**, 223–253.

McDonough W. F. and Yoshizaki T. (in press) Terrestrial planet compositions controlled by accretion disk magnetic field. *Prog. Earth Planet. Sci.*. doi.10.1186/s40645-021-00429-4.

Misawa K. and Nakamura N. (1988) Demonstration of REE fractionation among individual chondrules from the Allende (CV3) chondrite. *Geochim. Cosmochim. Acta* **52**, 1699–1710.

Misawa K. and Nakamura N. (1988) Highly fractionated rare-earth elements in ferromagnesian chondrules from the Felix (CO3) meteorite. *Nature* **334**, 47–50.

Morbidelli A., Libourel G., Palme H., Jacobson S. A. and Rubie D. C. (2020) Subsolar Al/Si and Mg/Si ratios of non-carbonaceous chondrites reveal planetesimal formation during early condensation in the protoplanetary disk. *Earth Planet. Sci. Lett.* **538**, 116220.

Münker C., Fonseca R. O. C. and Schulz T. (2017) Silicate Earth's missing niobium may have been sequestered into asteroidal cores. *Nat. Geosci.* **10**, 822–826.

Münker C., Pfänder J. A., Weyer S., Büchl A., Kleine T. and Mezger K. (2003) Evolution of planetary cores and the Earth-Moon system from Nb/Ta systematics. *Science* **301**, 84–87.

Namur O., Charlier B., Holtz F., Cartier C. and McCammon C. (2016) Sulfur solubility in reduced mafic silicate melts: Implications for the speciation and distribution of sulfur on Mercury. *Earth Planet. Sci. Lett.* **448**, 102–114.

Nebel O., van Westrenen W., Vroon P. Z., Wille M. and Raith M. M. (2010) Deep mantle storage of the Earth's missing niobium in late-stage residual melts from a magma ocean. *Geochim. Cosmochim. Acta* **74**, 4392–4404.

Nesbitt R. W., Sun S. S. and Purvis A. C. (1979) Komatiites; geochemistry and genesis. *Can. Mineral.* **17**, 165–186.

Nittler L. R., Chabot N. L., Grove T. L. and Peplowski P. N. (2018) The Chemical Composition of Mercury. In *Mercury: The View after MESSENGER* (eds. S. C. Solomon, L. R. Nittler and B. J. Anderson). Cambridge University Press, Cambridge, pp. 30–51.

Nittler L. R., Frank E. A., Weider S. Z., Crapster-Pregont E., Vorburger A., Starr R. D. and Solomon S. C. (2020) Global major-element maps of Mercury from four years of MESSENGER X-Ray Spectrometer observations. *Icarus*, 113716.

Nittler L. R., Starr R. D., Weider S. Z., McCoy T. J., Boynton W. V., Ebel D. S., Ernst C. M., Evans L. G., Goldsten J. O., Hamara D. K., Lawrence D. J., McNutt R. L., Schlemm C. E., Solomon S. C. and Sprague A. L. (2011) The major-element composition of Mercury's surface from MESSENGER X-ray spectrometry. *Science* **333**, 1847–1850.

Osborn T. W., Smith R. H. and Schmitt R. A. (1973) Elemental composition of individual chondrules from ordinary chondrites. *Geochim. Cosmochim. Acta* **37**, 1909–1942.

Pack A., Russell S. S., Shelley J. M. G. and Van Zuilen M. (2007) Geo- and cosmochemistry of the twin elements yttrium and holmium. *Geochim. Cosmochim. Acta* **71**, 4592–4608.

Pack A., Shelley J. M. G. and Palme H. (2004) Chondrules with peculiar REE patterns: Implications for solar nebular condensation at high C/O. *Science* **303**, 997–1000.

Palme H., Larimer J. W. and Lipschutz M. E. (1988) Moderately volatile elements. In *Meteorites and the Early Solar System* (eds. J. F. Kerridge and M. S. Matthews). The University of Arizona Press, Tucson, pp. 436–461.

Palme H. and O'Neill H. S. C. (2014) Cosmochemical estimates of mantle composition. In *Treatise on Geochemistry (second ed.)*, vol. 3 (eds. H. D. Holland and K. K. Turekian). Elsevier, Oxford, pp. 1–39.

Palme H., Spettel B. and Hezel D. (2014) Siderophile elements in chondrules of CV chondrites. *Chemie der Erde-Geochem.* **74**, 507–516.

Pasek M. A., Milsom J. A., Ciesla F. J., Lauretta D. S., Sharp C. M. and Lunine J. I. (2005) Sulfur chemistry with time-varying oxygen abundance during Solar System formation. *Icarus* **175**, 1–14.

Patzer A., Hezel D. C., Bendel V. and Pack A. (2018) Chondritic ingredients: II. Reconstructing early solar system history via refractory lithophile trace elements in individual objects of the Leoville CV3 chondrite. *Meteor. Planet. Sci.* **53**, 1391–1412.

Patzer A., Pack A. and Gerdes A. (2010) Zirconium and hafnium in meteorites. *Meteor. Planet. Sci.* **45**, 1136–1151.

Peplowski P. N., Evans L. G., Hauck S. A., McCoy T. J., Boynton W. V., Gillis-Davis J. J., Ebel D. S., Goldsten J. O., Hamara D. K., Lawrence D. J., McNutt R. L., Nittler L. R., Solomon S. C., Rhodes E. A., Sprague A. L., Starr R. D. and Stockstill-Cahill K. R. (2011) Radioactive elements on Mercury's surface from MESSENGER: Implications for the planet's formation and evolution. *Science* **333**, 1850–1852.

Piani L., Marrocchi Y., Libourel G. and Tissandier L. (2016) Magmatic sulfides in the porphyritic chondrules of EH enstatite chondrites. *Geochim. Cosmochim. Acta* **195**, 84–99.

Quirico E., Bourot-Denise M., Robin C., Montagnac G. and Beck P. (2011) A reappraisal of the metamorphic history of EH3 and EL3 enstatite chondrites. *Geochim. Cosmochim. Acta* **75**, 3088–3102.

Rambaldi E. R. and Wasson J. T. (1981) Metal and associated phases in Bishunpur, a highly unequilibrated ordinary chondrite. *Geochim. Cosmochim. Acta* **45**, 1001–1015.

Rambaldi E. R. and Wasson J. T. (1984) Metal and associated phases in Krymka and Chainpur: Nebular formational processes. *Geochim. Cosmochim. Acta* **48**, 1885–1897.

Rubie D. C., Frost D. J., Mann U., Asahara Y., Nimmo F., Tsuno K., Kegler P., Holzheid A. and Palme H. (2011) Heterogeneous accretion, composition and core–mantle differentiation of the Earth. *Earth Planet. Sci. Lett.* **301**, 31–42.

Rubie D. C., Jacobson S. A., Morbidelli A., O'Brien D. P., Young E. D., de Vries J., Nimmo F., Palme H. and Frost D. J. (2015) Accretion and differentiation of the terrestrial planets with implications for the compositions of early-formed Solar System bodies and accretion of water. *Icarus* **248**, 89–108.

Rubin A. E., Scott E. R. D. and Keil K. (1997) Shock metamorphism of enstatite chondrites. *Geochim. Cosmochim. Acta* **61**, 847–858.

Rudnick R. L., Barth M., Horn I. and McDonough W. F. (2000) Rutile-bearing refractory eclogites: Missing link between continents and depleted mantle. *Science* **287**, 278–281.

Ruzicka A., Floss C. and Hutson M. (2012) Amoeboid olivine aggregates (AOAs) in the Efremovka, Leoville and Vigarano (CV3) chondrites: A record of condensate evolution in the solar nebula. *Geochim. Cosmochim. Acta* **79**, 79–105.

Satterwhite C. and Righter K. (2007) Petrographic Descriptions. *Antarctic Meteorite Newsletter* **30**, 18–30.

Schneider D. M., Symes S. J. K., Benoit P. H. and Sears D. W. G. (2002) Properties of chondrules in EL3 chondrites, comparison with EH3 chondrites, and the implications for the formation of enstatite chondrites. *Meteor. Planet. Sci.* **37**, 1401–1416.

Schönbächler M., Carlson R. W., Horan M. F., Mock T. D. and Hauri E. H. (2010) Heterogeneous accretion and the moderately volatile element budget of Earth. *Science* **328**, 884–887.

Sharp C. M. and Wasserburg G. J. (1995) Molecular equilibria and condensation temperatures in carbon-rich gases. *Geochim. Cosmochim. Acta* **59**, 1633–1652.

Steenstra E. S. and van Westrenen W. (2020) Geochemical constraints on core-mantle differentiation in Mercury and the aubrite parent body. *Icarus* **340**, 113621.

Stracke A., Palme H., Gellissen M., Münker C., Kleine T., Birbaum K., Günther D., Bourdon B. and Zipfel J. (2012) Refractory element fractionation in the Allende meteorite: Implications for solar nebula condensation and the chondritic composition of planetary bodies. *Geochim. Cosmochim. Acta* **85**, 114–141.

Sun S. S. and McDonough W. F. (1989) Chemical and isotopic systematics of oceanic basalts: Implications for mantle composition and processes. *Geol. Soc. Lond. Spec. Public.* **42**, 313–345.

Uesugi M., Sekiya M. and Nakamura T. (2008) Kinetic stability of a melted iron globule during chondrule formation. I. Non-rotating model. *Meteor. Planet. Sci.* **43**, 717–730.

Urey H. C. and Craig H. (1953) The composition of the stone meteorites and the origin of the meteorites. *Geochim. Cosmochim. Acta* **4**, 36–82.

Varela M. E., Sylvester P., Brandstätter F. and Engler A. (2015) Nonporphyritic chondrules and chondrule fragments in enstatite chondrites: Insights into their origin and secondary processing. *Meteor. Planet. Sci.* **50**, 1338–1361.

Wade J. and Wood B. J. (2001) The Earth's 'missing' niobium may be in the core. *Nature* **409**, 75–78.

Walker R. J., McDonough W. F., Honesto J., Chabot N. L., McCoy T. J., Ash R. D. and Bellucci J. J. (2008) Modeling fractional crystallization of group IVB iron meteorites. *Geochim. Cosmochim. Acta* **72**, 2198–2216.

Wänke H. and Dreibus G. (1994) Chemistry and accretion history of Mars. *Philos. Trans. Roy. Soc. Lond. Ser. A Math. Phys. Sci.* **349**, 285–293.

Warren P. H. (2011) Stable-isotopic anomalies and the accretionary assemblage of the Earth and Mars: A subordinate role for carbonaceous chondrites. *Earth Planet. Sci. Lett.* **311**, 93–100.

Wasson J. T. and Kallemeyn G. W. (1988) Compositions of chondrites. *Philos. Trans. Roy. Soc. Lond. Math. Phys. Eng. Sci.* **325**, 535–544.

Weisberg M. K. and Kimura M. (2012) The unequilibrated enstatite chondrites. *Chemie der Erde-Geochem.* **72**, 101–115.

Willig M. and Stracke A. (2019) Earth's chondritic light rare earth element composition: Evidence from the Ce–Nd isotope systematics of chondrites and oceanic basalts. *Earth Planet. Sci. Lett.* **509**, 55–65.

Willig M., Stracke A., Beier C. and Salters V. J. M. (2020) Constraints on mantle evolution from Ce-Nd-Hf isotope systematics. *Geochim. Cosmochim. Acta* **272**, 36–53.

Wipperfurth S. A., Guo M., Šrámek O. and McDonough W. F. (2018) Earth's chondritic Th/U: Negligible fractionation during accretion, core formation, and crust-mantle differentiation. *Earth Planet. Sci. Lett.* **498**, 196–202.

Wood B. J. and Kiseeva E. S. (2015) Trace element partitioning into sulfide: How lithophile elements become chalcophile and vice versa. *Am. Mineral.* **100**, 2371–2379.

Wood J. A. and Hashimoto A. (1993) Mineral equilibrium in fractionated nebular systems. *Geochim. Cosmochim. Acta* **57**, 2377–2388.

Wurm G., Trieloff M. and Rauer H. (2013) Photophoretic separation of metals and silicates: The formation of Mercury-like planets and metal depletion in chondrites. *Astrophys. J.* **769**, 78.

Yoshizaki T. and McDonough W. F. (2020) The composition of Mars. *Geochim. Cosmochim. Acta* **273**, 137–162.

Yoshizaki T. and McDonough W. F. (in press) Earth and Mars–distinct inner solar system products. *Geochemistry*. doi.10.1016/j.chemer.2021.125746.

Yoshizaki T., Nakashima D., Nakamura T., Park C., Sakamoto N., Ishida H. and Itoh S. (2019) Nebular history of an ultrarefractory phase bearing CAI from a reduced type CV chondrite. *Geochim. Cosmochim. Acta* **252**, 39–60.

Zanda B., Bourot-Denise M., Perron C. and Hewins R. H. (1994) Origin and metamorphic redistribution of silicon, chromium, and phosphorus in the metal of chondrites. *Science* **265**, 1846–1849.

Associate editor: Stefan Weyer